

Resistive wall mode stabilization by differential rotation in an analytic tokamak

C J Ham, C G Gimblett and S E Penington

EURATOM/CCFE Fusion Association, Culham Science Centre, Abingdon, Oxon,
OX14 3DB, UK.

E-mail: christopher.ham@ccfe.ac.uk

Abstract. It is well known that stabilization of the resistive wall mode (RWM) may allow fusion power to be significantly increased for a given magnetic field in advanced tokamak operation. The principle of stabilization of the RWM by rotation has been established both experimentally and theoretically. Recent experimental results have indicated stabilization of the RWM has been achieved with very small levels of rotation using balanced neutral beam injection. The framework of Connor *et al.* (Connor *et al.* 1988 *Phys. Fluids* **31** 577) is used to develop two ideal plasma analytic toroidal models where stepped pressure profiles and careful ordering of terms are used to simplify the analysis. The first model has one resonant layer in the plasma and two resistive walls and the second has two resonant layers and one resistive wall. The RWM can be stabilized with slow rotation ($\sim 0.5\%\Omega_A$, where Ω_A is the Alfvénic rotation frequency) of a secondary resistive wall. A secondary rotating resistive wall can only stabilize the plasma if a perfectly conducting wall at that location would stabilize the plasma. Differential rotation in the plasma is investigated by rotating two resonant layers in the plasma at different rates. It is found in this model that differential rotation of the outer resonant surface can stabilize the RWM, with no rotation required at the inner surface.

Submitted to: *Plasma Phys. Control. Fusion*

1. Introduction

1.1. Background

A perfectly conducting tokamak wall is known to produce a stabilizing effect on the plasma. In fact, a perfect wall could increase the permissible stable β (where $\beta = 2\mu_0 p_0/B_0^2$ is the ratio of plasma pressure, p_0 , to magnetic pressure, and B_0 is the equilibrium magnetic field) by around 40%, see Reimerdes *et al.* [1] or Hender *et al.* [2], with the consequence that fusion power could be approximately doubled. In reality, the tokamak wall has a finite conductivity and so unstable modes can grow at a rate comparable to τ_w^{-1} , where τ_w is the vertical field diffusion time through the wall. These modes are called resistive wall modes (RWMs).

It is well known that experimental results have demonstrated that the RWM can be stabilized by rotation, see for example Reimerdes *et al.* [1]. This can be explained by one of the many RWM stabilization mechanisms that have been studied, for example: [3–8]. The levels of rotation match reasonably well between theory and experiment.

However, there is experimental evidence that the RWM has been stabilized even with very slow rotation, Reimerdes *et al.* [9, 10]. This might be explained by plasma resonances with ions, for example precessional drift resonance [11]. It is known that Coriolis and centrifugal forces can also act to reduce the growth rate of resistive wall modes, see Chu *et al.* [12] or Gimblett *et al.* [13]. These effects will not be considered further here. However, it is clear experimentally that the toroidal plasma rotation has a non-constant radial profile, [10] and this may provide another explanation as suggested in [9, 10, 14].

Differential rotation stabilization will be explored initially using the idea of a secondary rotating wall first developed for the reversed field pinch [15] and then analysed in a cylindrical tokamak geometry in [16]. The latter paper showed that the RWM could be stabilized in certain circumstances with no plasma rotation. The insight gained from the secondary rotating wall outside the plasma motivates investigation of a second differentially rotating resonant layer inside the plasma.

1.2. Overview

A toroidal analytic magnetohydrodynamic (MHD) stability model of a tokamak with circular cross section and large aspect ratio will be used here, as developed in Ham *et al.* [17]. Adjacent poloidal Fourier harmonics $\exp(im\theta)$, where θ is poloidal angle and m is poloidal mode number, are coupled together by toroidicity, so the m harmonic is just coupled to the $m - 1$ and $m + 1$ harmonics. An analytical treatment is made possible by the use of stepped equilibrium pressure and current profiles. In particular, the pressure steps have been located near to the rational surfaces which produces certain ‘magnifying factors’ (to be explained in more detail below) that are used to rank terms in deriving the model equations.

Background for the cylindrical and toroidal models will be given in section 2. Jump

conditions are required to connect solutions at the pressure steps and these will be given in section 3. The two RWM stabilization models will then be investigated. The first model, in section 4, has one resonance in the plasma and two resistive walls that can rotate at different rates outside. The second model, in section 5, has two resonant layers in the plasma which may rotate at different rates and one resistive wall outside. Conclusions and discussion will be given in section 6.

2. Background

2.1. Cylindrical model

In the cylindrical model, perturbed marginal force balance equation is used to model the stability of the plasma. This results in an equation for the perturbed poloidal magnetic flux ψ [5]

$$\frac{1}{r} \frac{d}{dr} \left(r \frac{d\psi}{dr} \right) - \frac{m^2}{r^2} \psi - \left(\frac{m\mu_0 J'_0}{rF_0} + \frac{2\mu_0 m^2 B_{\theta 0}^2 p'_0}{B_0^2 r^3 F_0^2} \right) \psi = 0, \quad (1)$$

where $F_0 = (B_{\theta 0}/r)(m - nq)$, $'$ denotes the radial derivative and J_0 and p_0 are the equilibrium current and pressure respectively. B_0 and $B_{\theta 0}$ are the unperturbed toroidal and poloidal magnetic induction respectively, $q(r) = (rB_0)/(R_0 B_{\theta 0})$ is the safety factor profile, where R_0 is the major radius, and μ_0 is the permeability of free space. Equation (1) is singular at rational surfaces where $m = nq(r_s)$ (n, m are the toroidal and poloidal mode numbers). This means that resistive and other physical effects must be included in a layer surrounding the rational surface.

Equation (1) is solved in the regions outside of the resonant surfaces and the solutions are forced to be continuous across these resonant surfaces. There will be a jump in the derivative of the solution across the resonant surface which defines

$$\Delta'_s \equiv \left[\frac{r\psi'(r)}{\psi(r)} \right]_{r_s}, \quad (2)$$

where r_s is the radial location of the resonant surface.

The resistive wall cannot be represented using (1) either and an ‘inner’ solution must be calculated there using the pre-Maxwell equations, and a thin wall approximation [18],

$$\Delta'_w \equiv \left[\frac{r\psi'(r)}{\psi(r)} \right]_{r_w} = \gamma\tau_w, \quad (3)$$

where γ is the growth rate of the mode, τ_w is the vertical field diffusion time of the wall and

$$[f]_r = \lim_{\epsilon \rightarrow 0} (f(r + \epsilon) - f(r - \epsilon)). \quad (4)$$

2.2. Toroidal model

A model which includes toroidal effects in the calculation can be formulated using the model developed by Connor *et al.* [19]. This model is derived from the linearized

marginal ideal MHD equations

$$\begin{aligned}\nabla\tilde{p} &= \mathbf{j} \times \mathbf{B}_0 + \mathbf{J}_0 \times \mathbf{b}, \\ \mu_0\mathbf{j} &= \nabla \times \mathbf{b}, \\ \tilde{p} &= -\boldsymbol{\xi} \cdot \nabla p_0, \\ \mathbf{b} &= \nabla \times (\boldsymbol{\xi} \times \mathbf{B}_0),\end{aligned}\tag{5}$$

which represent perturbed marginal force balance, Ampère's law, the equation of state for the perturbed pressure, \tilde{p} , and the induction equation respectively. The equilibrium current, \mathbf{J}_0 , magnetic field, \mathbf{B}_0 , and plasma pressure, p_0 , satisfy $\mathbf{J}_0 \times \mathbf{B}_0 = \nabla p_0$, \mathbf{j} and \mathbf{b} are the perturbed current and magnetic field respectively and $\boldsymbol{\xi}$ is the plasma displacement.

It is possible to Fourier decompose equations (5) into poloidal harmonics, which yields an infinite set of coupled equations. The coupling can be reduced to immediately adjacent harmonics if a large aspect ratio and circular plasma cross-section are assumed. This system of equations was used to develop an analytic tokamak [17].

An analytically tractable model will be produced by using a stepped pressure profile. The equations are further simplified by producing a 'magnifying' factor which allows certain terms to be neglected. This factor appears when the pressure step location, r_p , and the rational surface are placed close together, so the factor $\kappa \equiv m - nq(r_p)$ is small in the pressure step region. This factor appears in the denominator and so acts as a magnifier in the equations from [19]. There is therefore no pressure-free coupling in this model and coupling only occurs at r_p . More details of this calculation are given in [17].

2.3. Layer physics including toroidal effects

Equation (1) in the cylindrical case or equations (5) in the toroidal case are used outside the resonant layer. The solutions to this equation couple the wall mode to the layer by marginal force balance. Inside the layer other physical effects are required such as resistivity. The ideal (or inertial) layer response will be used here [20]

$$\Delta_s(\gamma) = -\frac{\pi}{\gamma\tau_A},\tag{6}$$

where τ_A is the Alfvén time at the layer, based on B_0 . The effects of layer physics on the RWM has been investigated in [21]. The final RWM dispersion relation is formed by matching the solution inside and outside the layer

$$\Delta_s(\gamma) = \Delta'_s.\tag{7}$$

It was noted in [17] that toroidal effects produce an enhancement to the plasma inertia in the resonant layer, ρ_{eff} . The enhancement depends on which collisionality regime the plasma is in. These effects have been investigated by Shaing [22] using the Fitzpatrick-Aydemir model [23]. The effect was included in Ham *et al.* [17] and it was found that it could reduce the critical rotation required for stabilization of the RWM quite significantly.

3. Pressure step jump conditions

The analytic model used here is derived using a stepped pressure profile. The coupling between the harmonics of the perturbed poloidal magnetic flux only happens at these pressure step locations. The details of the calculation of the jump conditions for each of the perturbed magnetic flux harmonics was given in [17]. The jump conditions are

$$[r\psi'_m] = m\hat{\beta} \left((1+s)(\psi_{m+1} - \psi_{m-1}) + \frac{r\psi'_{m+1}}{(m+1)} + \frac{r\psi'_{m-1}}{(m-1)} \right), \quad (8)$$

$$[\psi_m] = 0, \quad (9)$$

$$[r\psi'_{m+1}] = \frac{(m+1)^2}{m}(1+s)\hat{\beta}\psi_m, \quad (10)$$

$$[\psi_{m+1}] = -\frac{(m+1)}{m}\hat{\beta}\psi_m, \quad (11)$$

$$[r\psi'_{m-1}] = -\frac{(m-1)^2}{m}(1+s)\hat{\beta}\psi_m, \quad (12)$$

$$[\psi_{m-1}] = -\frac{(m-1)}{m}\hat{\beta}\psi_m, \quad (13)$$

where $s = rq'(r_p)/q(r_p)$ is the magnetic shear and ψ_l is the perturbed poloidal magnetic flux for the l th harmonic. Care needs to be taken over the definition of pressure in these equations as pointed out in [17]. It is this local pressure that appears in the coupling parameter when deriving the pressure step jump conditions. The coupling parameter is

$$\hat{\beta} = \frac{R_0}{r_p} \frac{2p_L\mu_0q_0^2}{B_0^2} \frac{m}{m-nq(r_p)} \approx \frac{\beta_L}{\epsilon_p\kappa} \quad (14)$$

where $\epsilon_p = r_p/R_0$ is the inverse aspect ratio, $\kappa \equiv m - nq(r_p)$, $\beta_L = 2p_L\mu_0/B_0^2$ and p_L is the jump in pressure across the pressure step. A high β ordering will be used such that $\beta_L/\epsilon_p \sim O(\sqrt{\kappa})$. It was shown in [17] that this higher pressure ordering will produce a pressure driven kink mode.

There are jumps in the $m-1$, (13), and $m+1$, (11), harmonics themselves at the pressure step which are due to equilibrium Pfirsch-Schluter current sheets [24]. It should also be noted that (8) is unambiguous because the RHS can be shown to be continuous across $r = r_p$ even though all of the constituent parts are discontinuous.

Some effects of rotation can be investigated by giving the plasma a bulk rotation Ω_p with respect to the wall. If the ideal layer response is assumed then the following dispersion relation is solved

$$\Delta'_s = \Delta_m(\gamma) = -\frac{\pi}{(\gamma - i\Omega_p)\tau_A}, \quad (15)$$

and $\tau_w/\tau_A = 14000$ will be used as is typical in DIII-D experiments [1]. Alternatively, we may use Galilean invariance to specify a rotation at the wall so that $\Delta'_w = (\gamma - i\Omega_w)\tau_w$. However, this does not include Coriolis or centrifugal effects which appear as a result of plasma rotation.

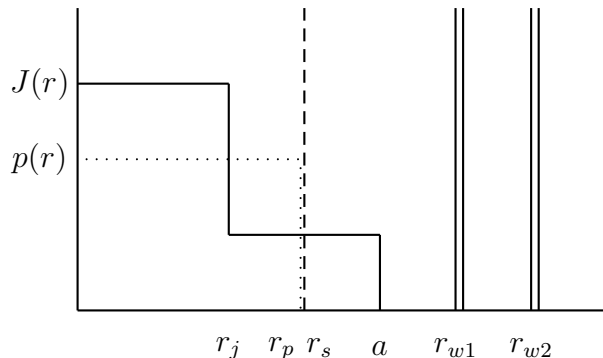


Figure 1. The current and pressure profile for the pressure driven kink mode with two resistive walls located at r_{w1} and r_{w2} .

4. Two walls one resonance

The idea of stabilizing the RWM in a fusion plasma using a secondary rotating resistive wall, first suggested in [15], arose in relation to reverse field pinches and has been applied to the line-tied cylindrical case by Hegna [25]. However, it has also been investigated in the tokamak configuration. Gimblett and Hastie [16] showed that in the case of a ‘cylindrical’ tokamak calculation, a suitably positioned secondary rotating wall outside the tokamak can stabilize the RWM at relatively low rotation rates even with a static plasma and first wall. A toroidal version of this calculation using the analytic toroidal model developed by Ham *et al.* [17] will be carried out here.

The plasma equilibrium that will be used for the two wall case is shown in figure 1. A specific set of parameters has been chosen to model a typical ideal pressure driven external kink mode with a resistive wall. The current profile is uniform either side of the two steps at $r_j = 0.5$ and $a = 1$. The ratio of the current density for $r_j < r < a$ to the current density for $r < r_j$ is $\zeta = 0.4$. The resistive wall is located at $r_w = 1.15$. The pressure step is at $r_p = 0.9$ and the rational surface just outside at $r_p + \epsilon = 0.905$. A ‘cartoon’ of the equilibrium is shown in figure 1. The poloidal mode number of the central harmonic is $m = 2$. The safety factor profile is flat for $r \leq r_j$ with $q(0) = 1.166$ and monotonically increasing for $r > r_j$ with $q(a) = 2.121$. The full toroidal problem is solved by matching the solutions in each region together using the jump conditions at the pressure and current steps and at the wall. The no wall stability limit of this equilibrium is $\hat{\beta} = 2.4574$ and the perfect wall limit is $\hat{\beta} = 7.9254$. It has been shown in Ham *et al.* [17] that with one wall this configuration produces a pressure driven kink mode.

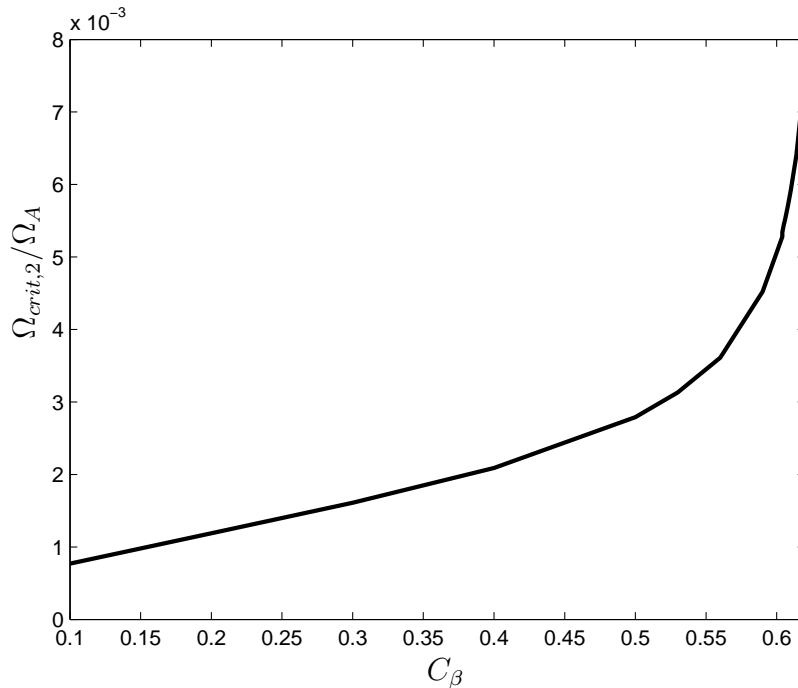


Figure 2. The critical rotation of the second wall required to stabilize the RWM against increasing pressure. The first wall is located at $r_{w1} = 1.15$ and the second wall is at $r_{w2} = 1.20$. The first wall and plasma are assumed static.

Figure 2 shows how the critical rotation for stabilization of the RWM changes with the pressure instability drive parameter C_β introduced by Reimerdes *et al.* [1]

$$C_\beta = \frac{\beta - \beta_{\text{No wall}}}{\beta_{\text{Perfect wall}} - \beta_{\text{No wall}}}. \quad (16)$$

Here $\beta_{\text{No wall}}$ is the no wall β limit and $\beta_{\text{Perfect wall}}$ is the perfect wall β limit. C_β is defined with reference to a perfect wall located at the first wall, r_{w1} . Relatively slow rotation of the secondary wall ($\sim 0.5\%\Omega_A$) is required for stabilization when the plasma and the first wall are assumed to be static. No inertial enhancement in the layer has been used in this calculation. Figure 2 shows a very sharp increase in critical rotation as $C_\beta \rightarrow 0.65$ because the secondary wall β limit corresponds to a first wall $C_\beta \approx 0.65$ and so second wall stabilization is impossible beyond this pressure limit.

The location of the second wall with respect to the first wall has been investigated and figure 3, which plots critical rotation for stabilization against the position of the second wall, shows that there is an optimum position for the second wall. If the second wall is withdrawn from the first wall the critical rotation first falls to a minimum at $r_{w2} \approx 1.05r_{w1}$ and then increases until the second wall is beyond the point where a perfect wall would stabilize the plasma. The second wall has no stabilizing effect beyond that point. A similar result is seen for the cylindrical case in Gimblett and Hastie [16].

A secondary rotating tokamak wall could in principle be realised by using a flowing lithium blanket [15]. The Wisconsin rotating wall machine [26, 27] is a line-

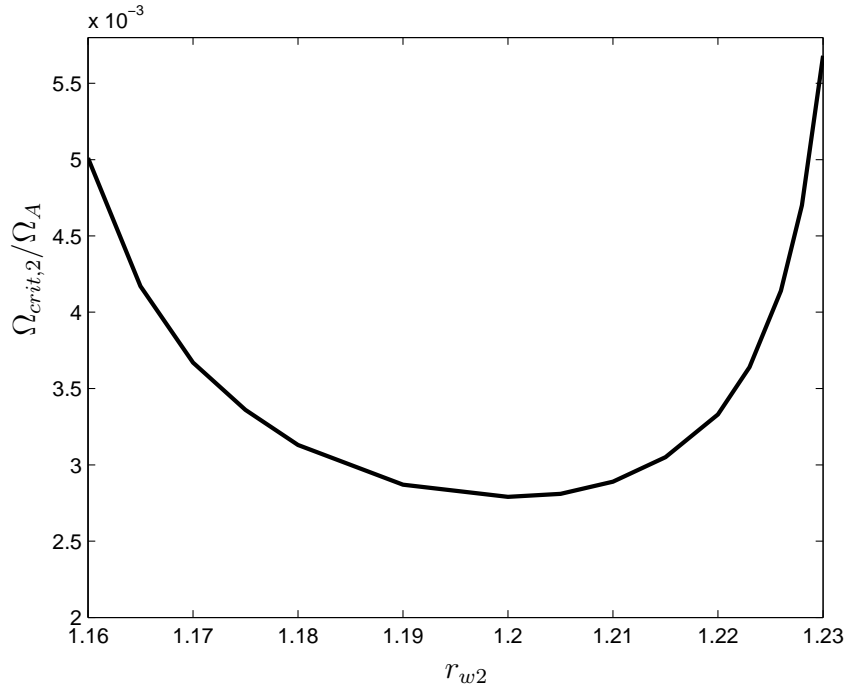


Figure 3. The critical rotation of the second wall required to stabilize the RWM for different second wall positions. First wall position is fixed at $r_{w1} = 1.15$.

tied cylindrical pinch experiment designed to investigate a secondary rotating wall or flowing metal blanket. A secondary rotating wall could also be ‘faked’ using an array of external coils, as investigated by Jensen and Fitzpatrick [28].

5. Two resonance pressure driven kink mode

In this section an equilibrium with two resonant surfaces and one resistive wall will be investigated. It is conjectured that a second resonance might act in a similar way to a second wall and facilitate RWM stabilization.

The equilibrium considered here is shown in figure 4. There are two pressure steps and two resonances at $q = m$ and $q = m + 1$, $m = 2$ will be used here. This means that four poloidal harmonics will be required. The details of the equilibrium used will now be given. The first current step is at $r_j = 0.5$, the edge of the plasma $a = 1$ and the ratio of the current density at the core to the edge is $\zeta = 0.4$. The inner pressure step is located at $r_{p1} = 0.55$ with the rational surface just outside it at $r_{s1} = 0.555$. The outer pressure step is located at $r_{p2} = 0.8805$ with rational surface just outside at $r_{s2} = 0.8855$. The ratio of the pressure jumps at the pressure steps is kept constant at $\beta_1/\beta_2 = 1.5$. The safety factor on axis is $q_0 = 1.7740$ and the safety factor at the plasma edge is $q_a = 3.2254$.

Figure 5 shows the four poloidal harmonics for the case with two resonant layers. Note that the $m - 1$ harmonic is small in comparison to the others and it has little

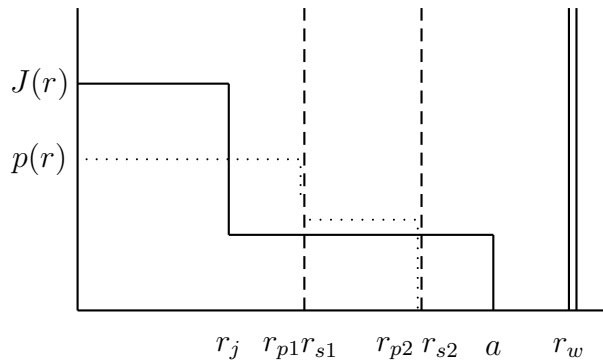


Figure 4. Current and pressure profile for the pressure driven kink mode with two internal resonant layers at r_{s1} and r_{s2} and one resistive wall at r_w .

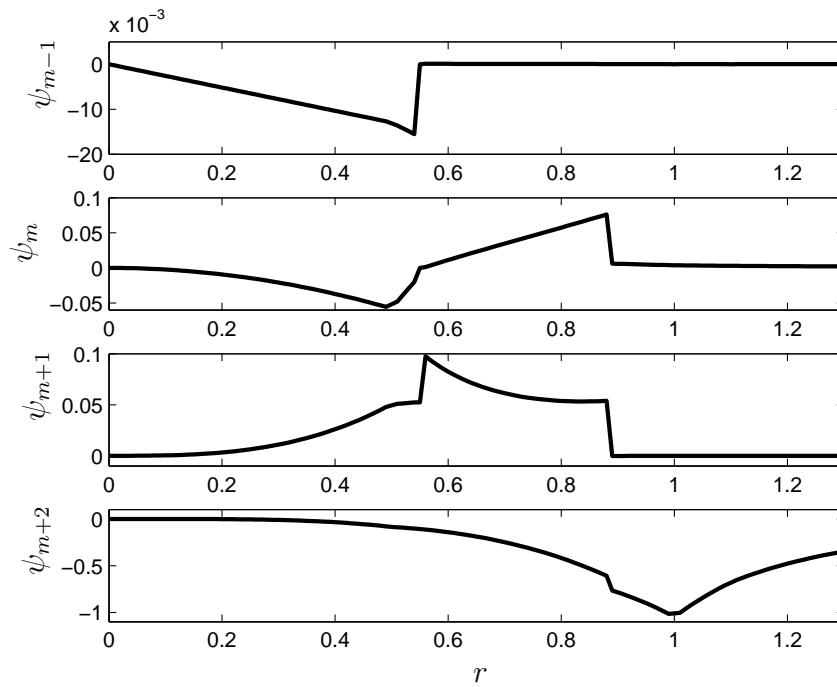


Figure 5. The four harmonics of the eigenfunction with two resonant surfaces. $C_\beta = 0.5$.

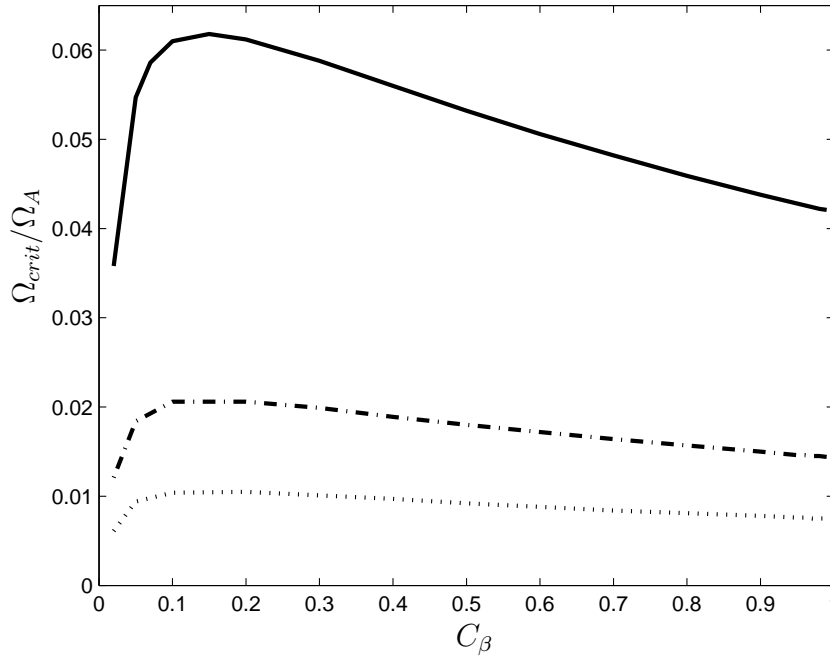


Figure 6. The rotation required to stabilize the RWM with no differential rotation against increasing pressure ($\Omega_1 = \Omega_2$). The solid line has no enhanced inertia, the dash-dot line has $\tau_A^{\text{eff}} = 3$ and the dotted line has $\tau_A^{\text{eff}} = 6$. The ratio of pressure steps was held at $\beta_1/\beta_2 = 1.5$.

activity outside the first pressure step. The m and $m + 1$ harmonics are of similar amplitude. The $m + 2$ harmonic is large compared to the other harmonics and has significant amplitude outside the wall location.

The rotation required to stabilize the RWM with no differential rotation is shown in figure 6. This plot has a similar shape to the one resonance case reported in Ham *et al.* [17]. The critical rotation has been calculated for the no enhancement case and two different values of enhanced inertia, $\tau_A^{\text{eff}} = 3\tau_A$ and $\tau_A^{\text{eff}} = 6\tau_A$. The enhanced inertia reduces the critical rotation significantly.

The RWM can be stabilized with rotation only at the r_{s2} surface, with the wall and r_{s1} static. The magnitude of the rotation required at the $m + 1$ surface is similar to the rotation required for the no differential rotation case, see figure 7. Again the required rotation is reduced if enhanced inertia is included in the layer. In this case it is not possible to stabilize the RWM if r_{s1} rotates and r_{s2} and the wall are static.

The effect of changing the rotation rate of the first resonance can also be investigated. Figure 8 shows that the minimum critical rotation required at r_{s2} occurs at small values of $\Omega_1 \sim 0.25\%\Omega_A$. It should be noted that this is a relatively small effect only reducing the critical rotation from $\sim 5.3\%\Omega_A$ to $\sim 4.6\%\Omega_A$. The $m + 2$ harmonic has the dominant penetration into the wall and it is the rotation of the $m + 1$ resonance that most strongly acts to stabilize this harmonic.

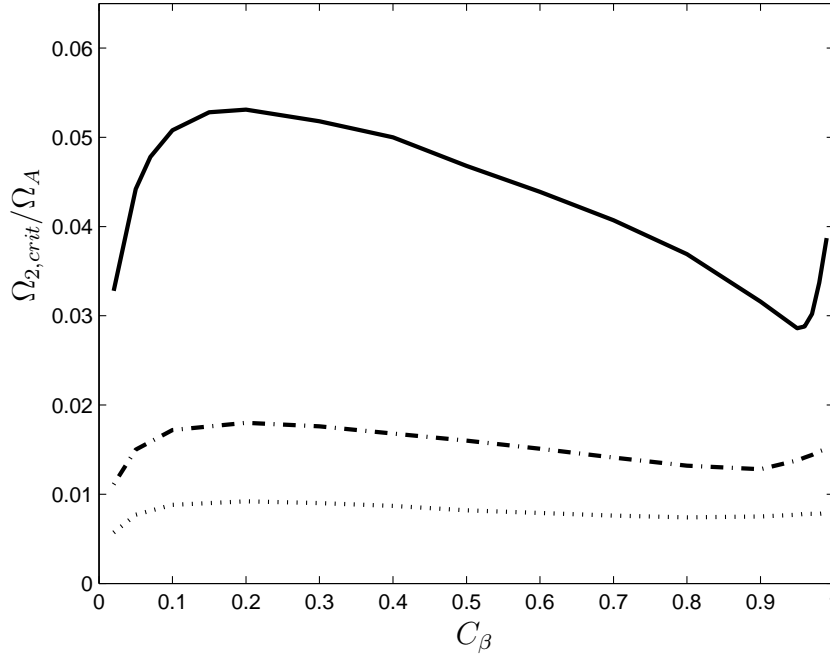


Figure 7. The rotation required to stabilize the RWM with differential rotation with increasing pressure ($\Omega_1 = 0, \Omega_2 \neq 0$). The solid line has no enhanced inertia, the dash-dot line has $\tau_A^{eff} = 3$ and the dotted line has $\tau_A^{eff} = 6$. The ratio of pressure steps was held at $\beta_1/\beta_2 = 1.5$.

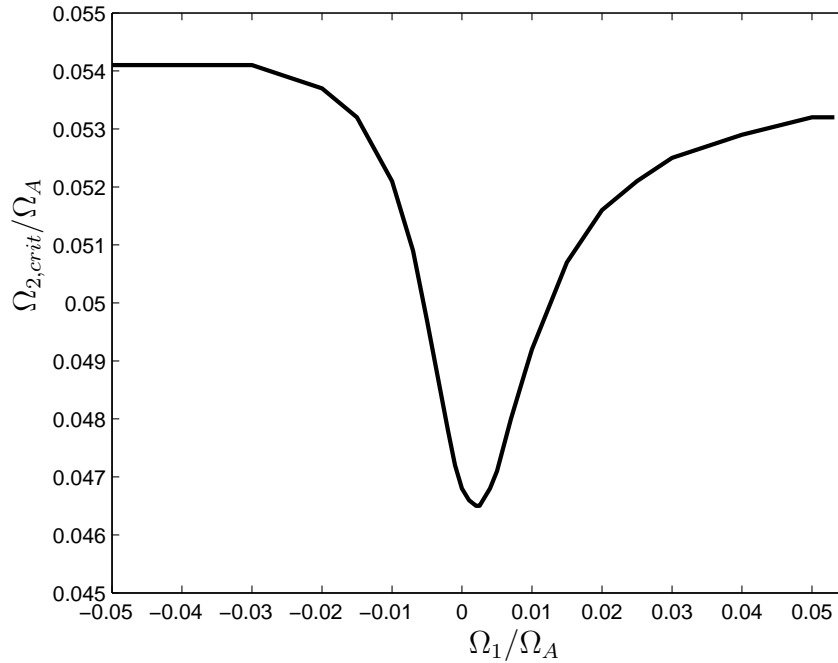


Figure 8. The rotation at the second resonance Ω_2 required for stabilization for different rates of rotation of the first resonance Ω_1 , with $C_\beta = 0.5$ and $\beta_1/\beta_2 = 1.5$. The wall is held static.

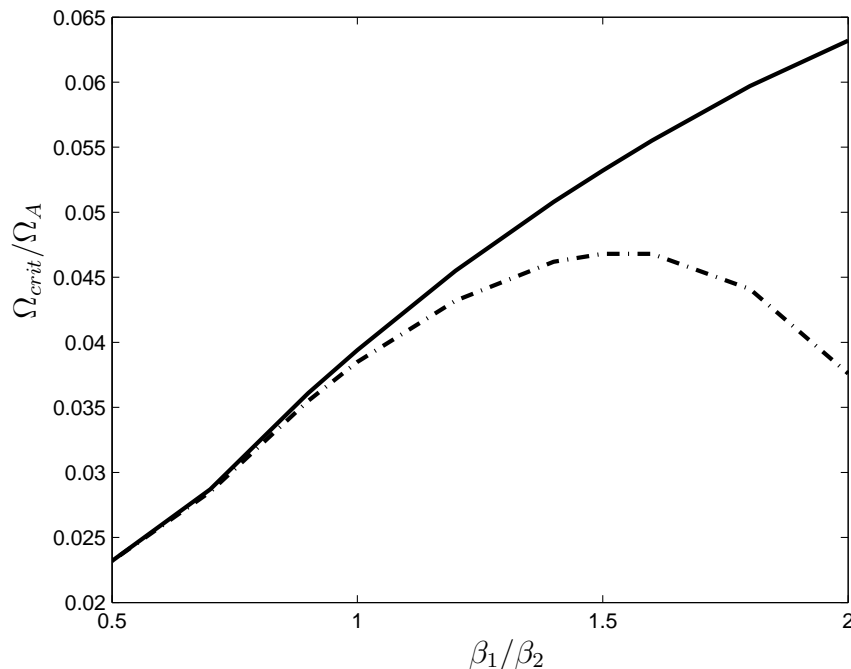


Figure 9. The effect of the relative pressure β_1/β_2 on the rotation required for stabilization with $C_\beta = 0.5$. The solid line assumes that there is no differential rotation ($\Omega_1 = \Omega_2$). The dashed line assumes $\Omega_1 = 0$ and only the second resonance is rotating.

The sensitivity of the pressure at each step β_1 and β_2 is shown in figure 9. For no differential rotation the critical rotation increases approximately linearly with β_1/β_2 . However, with differential rotation the critical rotation increases with β_1/β_2 at first and then reduces beyond $\beta_1/\beta_2 \sim 1.5$.

6. Discussion and Conclusions

Two models have been developed to investigate the effect of differential rotation on the stabilization of the toroidal RWM. The first model had one resonant layer in the plasma and two resistive walls outside. It was found that rotation of the second wall alone ($\sim 0.5\%\Omega_A$), with the plasma and first wall static, was sufficient to stabilize the RWM. The second wall has no effect outside the position where an ideal second wall would not stabilize the plasma. For maximum effect the second wall should be placed at $r_{w2} \approx 1.05r_{w1}$. It should be noted that a secondary rotating wall does not have to be literally that, it could be realised in principle using a flowing lithium blanket [15] or a suitable array of active coils [28].

A toroidal model for the resistive wall mode with two resonant surfaces in the plasma and one resistive wall outside has also been developed. The two resonant surfaces were rotated at different rates to investigate the suggestions made in [9, 14] that differential rotation could act to stabilize the RWM. It was found that the RWM

could be stabilized with rotation only of the r_{s2} surface, with the wall and core plasma static. There may be other effects if further resonant layers are included in the model.

If the main harmonic in this model is taken to be $m = 2$ and so $m + 1 = 3$, then the result in this paper may, in part, explain the results of experiments on RWM stability with balanced neutral beams. In these experiments the RWM is stable with little or no rotation at the $q = 2$ surface [9] when the mode would be expected to be unstable if differential rotation or kinetic effects were not considered.

Acknowledgments

It is a pleasure to acknowledge R J Hastie for useful discussions and T C Hender for helpful comments on the manuscript.

This work was funded by the RCUK Energy Programme under grant EP/I501045 and by the European Communities under the contract of association between EURATOM and CCFE. The views and opinions expressed herein do not necessarily reflect those of the European Commission.

References

- [1] Reimerdes H *et al.* 2006 *Phys. Plasmas* **13** 056107
- [2] Hender T C *et al.* 2007 *Nucl. Fusion* **47** S128–S202
- [3] Finn J M 1995 *Phys. Plasmas* **2** 198
- [4] Finn J M 1995 *Phys. Plasmas* **2** 3782
- [5] Bondeson A and Xie H X 1997 *Phys. Plasmas* **4** 2081
- [6] Bondeson A and Ward D J 1994 *Phys. Rev. Lett.* **72** 2709
- [7] Betti R and Freidberg J P 1995 *Phys. Rev. Lett.* **74** 2949
- [8] Bondeson A and Chu M S 1996 *Phys. Plasmas* **3** 3013
- [9] Reimerdes H *et al.* 2007 *Phys. Rev. Lett.* **98** 055001
- [10] Reimerdes H *et al.* 2007 *Plasma Phys. Control. Fusion* **49** B349
- [11] Hu B and Betti R 2004 *Phys. Rev. Lett.* **93** 105002
- [12] Chu M S *et al.* 1995 *Phys. Plasmas* **2** 2236
- [13] Gimblett C G *et al.* 1996 *Phys. Plasmas* **3** 3619
- [14] Sontag A C *et al.* 2007 *Nucl. Fusion* **47** 1005
- [15] Gimblett C G 1989 *Plasma Phys. and Control. Fusion* **31** 2183
- [16] Gimblett C G and Hastie R J 2000 *Phys. Plasmas* **7** 5007
- [17] Ham C J, Gimblett C G, and Hastie R J 2011 *Plasma Phys. Control. Fusion* **53** 025001
- [18] Gimblett C G 1986 *Nucl. Fusion* **26** 617
- [19] Connor J W *et al.* 1988 *Phys. Fluids* **31** 577
- [20] Porcelli F 1987 *Phys. Fluids* **30** 1734
- [21] Ham C J, Gimblett C G, and Hastie R J 2009 *Plasma Phys. Control. Fusion* **51** 115010
- [22] Shaing K C 2004 *Phys. Plasmas* **11** 5525
- [23] Fitzpatrick R and Aydemir A Y 1996 *Nucl. Fusion* **36** 11
- [24] Wesson J 1997 *Tokamaks* (Oxford: Oxford University Press)
- [25] C C Hegna 2004 *Phys. Plasmas* **11** 4230
- [26] Forest C B *et al.* 2000 *Bull. Am. Phys. Soc.* **45** 330
- [27] Bergerson W F *et al.* 2008 *Phys. Rev. Lett.* **101** 235005
- [28] Jensen T H and Fitzpatrick R 1996 *Phys. Plasmas* **3** 2641